



1 **Quantifying streamflow and active groundwater storage in response to climate**
2 **warming in an alpine catchment, upper Lhasa River**

3 Lu Lin^{a,b}, Man Gao^c, Jintao Liu^{a,b*}, Jiarong Wang^{a,b}, Shuhong Wang^{a,b*}, Xi Chen^{a,b,c},
4 Hu Liu^d

5 ^a *State Key Laboratory of Hydrology-Water Resources and Hydraulic Engineering,*
6 *Hohai University, Nanjing 210098, People's Republic of China*

7 ^b *College of Hydrology and Water Resources, Hohai University, Nanjing 210098,*
8 *People's Republic of China*

9 ^c *Institute of Surface-Earth System Science, Tianjin University, Tianjin 300072,*
10 *People's Republic of China*

11 ^d *Linze Inland River Basin Research Station, Chinese Ecosystem Research Network,*
12 *Lanzhou 730000, People's Republic of China*

13 * *Corresponding author. Tel.: +86-025-83787803; Fax: +86-025-83786606.*

14 *E-mail address: jtliu@hhu.edu.cn (J.T. Liu).*



15 **Abstract**

16 Climate warming is changing streamflow regimes and groundwater storage in cold
17 alpine regions. In this study, a headwater catchment named Yangbajain in the Lhasa
18 River Basin is adopted as the study area for quantifying streamflow changes and
19 active groundwater storage in response to climate warming. The changes in
20 streamflow regimes and climate factors are evaluated based on hydro-meteorological
21 observations from 1979 to 2013. The results show that annual streamflow increases
22 significantly at a rate of about 12.30 mm/10a during this period. Through baseflow
23 recession analysis, we also find that the estimated groundwater storage that is
24 comparable with the GRACE data increases significantly at the rates of about 19.32
25 mm/10a during these years. The rising of air temperature is the main factor for the
26 increase in streamflow and groundwater storage, which has led to a loss of over 25%
27 of the total glacier volume for half century in this catchment. Parallel comparisons
28 with other sub-basins in the Lhasa River Basin reveal that the increased streamflow at
29 the Yangbajain station is mainly fed by the accelerated glacier retreat rather than
30 frozen ground degradation. However, the increase of active storage capacity is caused
31 by frozen ground degradation, which can accommodate the increasing meltwater in
32 the valley. The huge gap between the melt-derived runoff and the increased water
33 volume in groundwater storage and streamflow suggests that more than 60% of the
34 total ablation of glaciers should be discharged downstream through deep fault. This
35 study provides a perspective to clarify the impact of glacial retreat and frozen ground



36 degradation on hydrological processes, which fundamentally affects the water supply
37 and the mechanisms of streamflow generation and change.
38 **Keywords:** Climate warming; Streamflow; Groundwater storage; Glacier retreat;
39 Frozen ground degradation; Tibetan Plateau



40 **1. Introduction**

41 Often referred to as the “Water Tower of Asia”, the Tibetan Plateau (TP) is the
42 source area of major rivers in Asia, e.g., the Yellow, Yangtze, Mekong, Salween, Indus,
43 and Brahmaputra Rivers (Cuo et al., 2014). The delayed release of water resources on
44 the TP through glacier melt can augment river runoff during dry periods, giving it a
45 pivotal role for water supply for downstream populations, agriculture and industries in
46 these rivers (Viviroli et al., 2007; Pritchard, 2017). However, the TP is experiencing a
47 significant warming period during the last half century (Kang et al., 2010; Liu and
48 Chen, 2000). Along with the rising temperature, major warming-induced changes
49 have occurred over the TP, such as glacier retreat (Yao et al., 2004; Yao et al., 2007)
50 and frozen ground degradation (Wu and Zhang, 2008). Hence, it is of great
51 importance to elucidate how climate warming influences hydrological processes and
52 water resources on the TP.

53 In cold alpine catchments, a glacier is known as a “solid reservoir” that supplies
54 water as streamflow, while frozen ground, especially permafrost, serves as an
55 impermeable barrier to the interaction between surface water and groundwater
56 (Immerzeel et al., 2010; Walvoord and Kurylyk, 2016). Since the 1990s, most glaciers
57 across the TP have retreated rapidly due to global warming and caused an increase of
58 more than 5.5% in river runoff from the plateau (Yao et al., 2007). Meltwater is the
59 key contributor to streamflow increase especially for headwater catchments with
60 larger glacier coverage (>5%) (Bibi et al., 2018). Meanwhile, in a warming climate,



61 numerous studies suggested that frozen ground on the TP has experienced a noticeable
62 degradation during the past decades (Cheng and Wu, 2007; Wu and Zhang, 2008).
63 Frozen ground degradation can modify surface conditions and change thawed active
64 layer storage capacity in the alpine catchments (Niu et al., 2011). Thawing of frozen
65 ground increases surface water infiltration, supports deeper groundwater flow paths,
66 and then enlarges groundwater storage, which is expected to have a profound effect
67 on flow regimes (Kooi et al., 2009; Bense et al., 2012; Walvoord and Striegl, 2007;
68 Woo et al., 2008; Ge et al., 2011; Walvoord and Kurylyk, 2016).

69 It is challenging to understand how glacier melt and frozen ground thaw alters the
70 mechanism of streamflow in a warmer climate due to the complicated interactions
71 between hydrological and cryospheric processes. In earlier phase of glacier melt,
72 accelerated glacier retreat will bring large quantities of meltwater available directly
73 for surface runoff or indirectly for groundwater recharge (Bayard et al., 2005).
74 Meanwhile, frozen ground thawing may allow for increased groundwater recharge
75 from meltwater infiltration (Evans and Ge, 2017). Generally, climate warming is
76 hypothesized to generate a quantitative and temporal shift in the partitioning of
77 meltwater between surface runoff and groundwater flow, and thereby alter the
78 quantity and timing of baseflow (Green et al., 2011; Evans et al., 2018). Through
79 groundwater modeling, Evans et al. (2015) found an increase in mean annual surface
80 temperature of 2 °C reduced approximately 28% of the areal extent of permafrost and
81 tripled baseflow contribution to streamflow in a headwater catchment on the northern



82 TP. Qin et al. (2016) discovered that the increasing precipitation and the thawing of
83 frozen ground were the main factors on the increase of baseflow with no significant
84 change in surface runoff in the upper Heihe River Basin of the northeastern TP.
85 Previous data-based studies indicated that the baseflow has increased especially
86 during winter with a reduction or no pervasive change in summer streamflow in the
87 central and northern TP (Liu et al., 2011; Niu et al., 2016) as well as Arctic rivers
88 (Walvoord and Striegl, 2007; Smith et al., 2007; St. Jacques and Sauchyn, 2009).
89 Moreover, based on numerical simulations, Bense et al. (2012) suggested that the
90 increasing groundwater storage caused by frozen ground degradation would delay
91 baseflow increase possibly by several decades to centuries. A slowdown in baseflow
92 recession was found in the northeastern and central TP (Niu et al., 2011; Niu et al.,
93 2016; Wang et al., 2017), in northeastern China (Duan et al., 2017), and in Arctic
94 rivers (Lyon et al., 2009; Lyon and Destouni, 2010; Walvoord and Kurylyk, 2016).

95 While, previous studies were important for understanding the effects of climate
96 warming on hydrological changes in cold alpine catchments (Niu et al., 2011; Niu et
97 al., 2016; Wang et al., 2017). However, quantitatively characterizing storage
98 properties and sensitivity to climate warming in cold alpine catchments is still
99 important for local water as well as downstream water management (Staudinger,
100 2017). Moreover, revealing the storage characteristics makes it easier to predict
101 hydrological cycle and streamflow changes response to a warming climate in cold
102 alpine catchments (Singleton and Moran, 2010). Thus, this study focuses on



103 quantifying streamflow and aquifer storage volume response to changes in glacier
104 melt and frozen ground thaw at the catchment scale on the southern TP. However, it is
105 difficult to directly measure catchment aquifer storage (Staudinger, 2017; Käser and
106 Hunkeler, 2016) and the GRACE data has low resolution and accuracy in assessing
107 total groundwater storage changes at the catchment scale (Green et al., 2011). An
108 alternative method, namely, recession flow analysis, can theoretically be used to
109 derive the active groundwater storage volume to reflect frozen ground degradation in
110 a catchment (Brutsaert and Nieber, 1977; Brutsaert, 2008). For example, the
111 groundwater storage changes can be inferred by recession flow analysis assuming
112 linearized outflow from aquifers into streams (Lin and Yeh, 2017). Due to the
113 complex structures and properties of catchment aquifers, the linear reservoir model
114 may not sufficient to represent the actual storage dynamics (Wittenberg, 1999;
115 Chapman, 1999; Liu et al., 2016). Hence, Lyon et al. (2009) adopted the nonlinear
116 reservoir to fit baseflow recession curves for the derivation of aquifer attributes,
117 which can be developed for inferring aquifer storage. Buttle (2017) used Kirchner's
118 (2009) approach for estimating the dynamic storage in different basins and found that
119 the storage and release of dynamic storage may mediate baseflow response to
120 temporal changes.

121 In this study, the Yangbajain Catchment in the Lhasa River Basin is adopted as the
122 study area. The catchment is experiencing glacier retreat and frozen ground
123 degradation in response to climate warming. The main objectives of this study are (1)



124 to quantify the changes between surface runoff and baseflow in a warming climate; (2)
125 to quantify active groundwater storage volume by recession flow analysis; (3) to
126 analyze the impacts of the changes in active groundwater storage on streamflow
127 variation. The paper is structured as follows. The section of Materials and Methods
128 includes the study area, data sources and methods. The Results and Discussion
129 sections present the changes in streamflow and its components, climate factors, and
130 glaciers, and we will discuss the changes in streamflow volume and baseflow
131 recession in response to the changes in active groundwater storage. The main
132 conclusions are summarized in the Conclusions section.

133 **2. Materials and Methods**

134 **2.1. Study area**

135 The 2,645 km² Yangbajain Catchment in the western part of the Lhasa River Basin
136 (Figure 1a) lies between the Nyainq&ntanglha Range to the northwest and the
137 Yarlu-Zangbo suture to the south. In the central of the catchment, a wide and flat
138 valley (Figure 1b) with low-lying terrain and thicker aquifers is in a half-graben
139 fault-depression basin caused by the Damxung-Yangbajain Fault (Wu and Zhao, 2006;
140 Yang et al., 2017). As a half graben system, the north-south trending
141 Damxung-Yangbajain Fault (Figure 1b) provides the access for groundwater flow as
142 manifested by the widespread distribution of hot springs (Jiang et al., 2016). The
143 surface of the valley is blanketed by Holocene-aged colluvium, filled with the great
144 thickness of alluvial-pluvial sediments from the south such as gravel, sandy loam, and



145 clay. The vegetation in the catchment is characteristic of alpine meadow, alpine steppe,
146 marsh, shrub, etc; meadow and marsh are mainly distributed in the valley and river
147 source (Zhang et al., 2010).

148 Located on the south-central TP, the Yangbajain Catchment is a glacier-fed
149 headwater catchment with significant frozen ground coverage (Figures 1b & 1c). A
150 majority of glaciers were found along the Nyainq̄ntanglha Ranges (Figure 1b).
151 Glaciers cover over ten percent of the whole catchment, making it the most
152 glacierized sub-basin in the Lhasa River Basin. According to the First Chinese Glacier
153 Inventory (Mi et al., 2002), the total glacier area was about 316.31 km² in 1960. The
154 ablation period of the glaciers ranges from June to September with the glacier termini
155 at about 5,200 m (Liu et al., 2011). According to the new map of permafrost
156 distribution on the TP (Zou et al., 2017), the valley is underlain by seasonally frozen
157 ground (Figure 1c). It is estimated that seasonally frozen ground and permafrost
158 accounts for about 64% and 36% of the total catchment area, respectively (Zou et al.,
159 2017). The lower limit of alpine permafrost is around 4,800 m, and the thickness of
160 permafrost varies from 5 m to 100 m (Zhou et al., 2000).

161 The catchment is characterized by a semi-arid temperate monsoon climate. The
162 average annual air temperature of the Yangbajain Catchment is approximately -2.3 °C
163 with monthly variation from -8.6 °C in January to 3.1 °C in July (Figure 2). The
164 average annual precipitation at the Yangbajain Station in the valley is about 427 mm.
165 The catchment has a summer (June-August) monsoon with 73% of the yearly



166 precipitation, while the rest of the year is dry with only 1% of the yearly precipitation
167 occurring in winter (December-February) (Figure 2).

168 The average annual streamflow is 277.7 mm, and the intra-annual distribution of
169 streamflow is uneven (Figure 2). In summer, streamflow is recharged mainly by
170 monsoon rainfall and meltwater, which accounts for approximately 63% of the yearly
171 streamflow (Figure 2). The streamflow in winter with only 4% of the yearly
172 streamflow (Figure 2) is only recharged by groundwater, which is greatly affected by
173 the freeze-thaw cycle of frozen ground and the active layer (Liu et al., 2011).

174 **2.2. Data**

175 Daily streamflow and precipitation data at the four hydrological Stations (Figure 1a)
176 during the period 1979-2013 are collected from the Tibet Autonomous Region
177 Hydrology and Water Resources Survey Bureau. The monthly meteorological data at
178 the three weather stations (Figure 1a) are obtained from the China Meteorological
179 Data Sharing Service System (<http://data.cma.cn/>) for the years from 1979 to 2013. In
180 this study, the method of meteorological data extrapolation by Prasch et al. (2013) is
181 adopted to obtain the discretized air temperature (with cell size as 1 km×1 km) of
182 the Lhasa River Basin based on the air temperature of the three stations assuming a
183 linear lapse rate. The mean monthly lapse rate is set to 0.44 °C/100m for elevations
184 below 4,965 m and 0.78 °C/100m for elevations above 4,965 m in the catchment
185 (Wang et al., 2015).

186 The glaciers and frozen ground data are provided by the Cold and Arid Regions



187 Science Data Center (<http://westdc.westgis.ac.cn/>). The distribution, area and volume
188 of glaciers are based on the First and Second Chinese Glacier Inventory in 1960 and
189 2009 (Mi et al., 2002; Liu et al., 2014) (Figure 1b). The distribution and classification
190 of frozen ground (Figure 1c) are collected from the twice maps of frozen ground on
191 the TP (Li and Cheng, 1996; Zou et al., 2017).

192 The latest Level - 3 monthly mascon solutions (CSR, Save et al., 2016) was used to
193 detect terrestrial water storage (TWS, total vertically-integrated water storage)
194 changes for the period from January 2003 to December 2015 with spatial sampling of
195 $0.5^{\circ} \times 0.5^{\circ}$ from the Gravity Recovery and Climate Experiment (GRACE) satellite.
196 The time series of 2003~2015 for snow water equivalent (SWE), total soil moisture
197 (SM, layer 0~200cm) from the dataset (GLDAS_Noah2.1, <https://disc.gsfc.nasa.gov/>)
198 were adopted for derivation of the groundwater storage (GWS) (Richey et al., 2015).

199 **2.3. Methods**

200 *2.3.1. Statistical methods for assessing streamflow changes*

201 The Mann-Kendall (MK) test, which is suitable for data with non-normally
202 distributed or nonlinear trends, is applied to detect trends of hydro-meteorological
203 time series (Mann, 1945; Kendall, 1975). To remove the serial correlation from the
204 examined time series, a Trend-Free Pre-Whitening (TFPW) procedure is needed prior
205 to applying the MK test (Yue et al., 2002). A more detailed description of the
206 Trend-Free Pre-Whitening (TFPW) approach was provided by Yue et al. (2002).

207 Gray relational analysis was aimed to find the major climatic or hydrological



208 factors that influenced an objective variable (Liu et al., 2005; Wang et al., 2013). In
209 this paper, gray relational analysis is used to investigate the main climatic factor
210 impacting the streamflow.

211 2.3.2. Baseflow separation

212 In this paper, the most widely used one-parameter digital filtering algorithm is
213 adopted for baseflow separation (Lyne and Hollick, 1979). The filter equation is
214 expressed as

$$215 \quad q_t = \alpha q_{t-1} + \frac{1+\alpha}{2}(Q_t - Q_{t-1}) \quad (1)$$

$$216 \quad b_t = Q_t - q_t \quad (2)$$

217 where q_t and q_{t-1} are the filtered quick flow at time step t and $t-1$, respectively; Q_t and
218 Q_{t-1} are the total runoff at time step t and $t-1$; α is the filter parameter, ranging from
219 0.9 to 0.95; b_t is the filtered baseflow.

220 2.3.3. Determination of active groundwater storage

221 The method of recession flow analysis is widely used to investigate the baseflow
222 recession characteristics and the storage-discharge relationship of catchments (Lyon et
223 al., 2009; Lyon and Destouni, 2010; Sjöberg et al., 2013; Lin and Yeh., 2017; Gao et
224 al., 2017). Physical considerations based on hydraulic groundwater theory suggest
225 that the groundwater storage in a catchment can be approximated as a power function
226 of baseflow rate at the catchment outlet (Brutsaert, 2008)

$$227 \quad S = Ky^m \quad (8)$$

228 where S is the volume of active groundwater storage (abbreviated as groundwater



229 storage in the following context) in the catchment aquifers (see in Figure 3). The
230 active groundwater storage S is defined as the storage that controls streamflow
231 dynamics assuming that streamflow during rainless periods is a function of catchment
232 storage (Kirchner, 2009; Staudinger, 2017); K , m are constants depending on the
233 catchment physical characteristics, and K is the baseflow recession coefficient,
234 represented the time scale of the catchment streamflow recession process; y is the rate
235 of baseflow in the stream.

236 During dry season without precipitation and other input events, the flow in a stream
237 can be assumed to depend solely on the groundwater storage from the upstream
238 aquifers (Brutsaert, 2008; Lin and Yeh, 2017). For such baseflow conditions, the
239 conservation of mass equation can be represented as

$$240 \quad \frac{dS}{dt} = -y \quad (9)$$

241 where t is the time. Substitution of equation (8) in equation (9) yields (Brutsaert and
242 Nieber, 1977)

$$243 \quad -\frac{dy}{dt} = ay^b \quad (10)$$

244 where dy/dt is the temporal change of the baseflow rate during recessions, and the
245 constants a and b are called the recession intercept and recession slope of plots of
246 $-dy/dt$ versus y in log-log space, respectively. The parameters of K and m in equation
247 (8) can be expressed by a and b , where $K = 1/[a(2-b)]$ and $m = 2-b$ (Gao et al.,
248 2017). In the storage discharge relationship, the aquifer responds as a linear reservoir
249 if $b=1$, and as nonlinear reservoir if $b \neq 1$.



250 In our study, the baseflow recession data are selected from the streamflow
251 hydrographs, which remarkably decline for at least 3 days after rainfall ceases and
252 remove the first 2 days to avoid the impact of storm flow (Brutsaert and Lopez, 1998).
253 A variable time interval Δt is used to properly scale the observed drop in streamflow
254 to avoid discretization errors on $-dy/dt \sim y$ plot due to measurement noise, especially in
255 the log-log space (Rupp and Selker, 2006; Kirchner, 2009). Then the constants a and b
256 are fitted by using a nonlinear least squares regression through all data points of
257 $-dy/dt$ versus y in log-log space for all years to avoid the difficulty of defining a lower
258 envelop of the scattered points (Lyon et al., 2009). Theoretically, one can fit a line of
259 slope b to recession flow data graphed in this manner and determine aquifer
260 characteristics from the resulting value of a (Rupp and Selker, 2006). That is to say,
261 with a fixed slope b during recessions, it should be possible to observe the changes in
262 catchment aquifer properties by fitting the intercept a as a variable across different
263 years. Since the values of K and m can be calculated by fitting recession intercept a
264 and the fixed slope b , the average groundwater storage S for dry season can be
265 obtained through equation (8) based on average rate of baseflow.

266 3. Results

267 3.1. Assessment of streamflow changes

268 The annual streamflow of the Yangbajain Catchment shows an increasing trend at
269 the 5% significance level with a mean rate of about 12.30 mm/10a over the period
270 1979-2013 (Table 1 and Figure 4a). Meanwhile, annual mean air temperature exhibits



271 an increasing trend at the 1% significance level with a mean rate of about 0.28 °C/10a
272 (Table 1 and Figure 5a). However, annual precipitation has a nonsignificant trend
273 during this period (Table 1 and Figure 5b).

274 As annual streamflow increases significantly, it is necessary to analyze to what
275 extent the changes in the two components (quick flow and baseflow) lead to
276 streamflow increases. Based on the baseflow separation method, the annual mean
277 baseflow contributes about 59% of the annual mean streamflow in the catchment. The
278 MK test shows that annual baseflow exhibits a significant increasing trend at the 1%
279 level with a mean rate of about 10.95 mm/10a over the period 1979-2013 (Table 1 and
280 Figure 4b). But the trend is statistically nonsignificant for annual quick flow in the
281 same period (Table 1). The increasing trends between the baseflow and streamflow
282 are very close, indicating that the increase in baseflow is the main contributor to
283 streamflow increases.

284 Furthermore, gray relational analysis is applied to the catchment to identify the
285 major climatic factors for the increasing streamflow. The result shows that the air
286 temperature has the higher gray relational grade at annual scale (Table 2). This
287 indicates that the air temperature acts as a primary factor for the increased streamflow
288 as well as the baseflow.

289 The annual streamflow and baseflow significantly increase due to the rising air
290 temperature over the period 1979-2013. However, there are diverse intra-annual
291 variation characteristics for streamflow as well as the two streamflow components



292 during the period. Streamflow in spring (March to May), autumn (September to
293 November) and winter (December to February) show increasing trends at least at the
294 5% significance level (Figure 6a, 6c and 6d), while streamflow in summer (June to
295 August) has a nonsignificant trend during this period (Figure 6b). Baseflow also
296 increases significantly in spring, autumn and winter (Figure 6a, 6c and 6d). The trend
297 is statistically nonsignificant for baseflow in summer (Figure 6b). Quick flow exhibits
298 nonsignificant trend for all seasons (Table 1). As to the meteorological factors, mean
299 air temperature in all seasons increase significantly at the 1% level especially during
300 winter with the rate of about 0.51 °C/10a (Table 1 and Figure 7), whereas precipitation
301 in each season shows nonsignificant trend during these years (Table 1). The gray
302 relational analysis shows that the air temperature is the critical climatic factor for the
303 changes in streamflow and baseflow in all seasons (Table 2).

304 Compared with monsoon rainfall as the main water source for summer runoff, the
305 corresponding contribution of glacial meltwater to the streamflow only accounts for
306 max. 11% in the catchment (Prasch et al., 2013). Moreover, the summer meltwater
307 partly infiltrates into soils and will be stored in aquifers. This can explain why it is
308 statistically nonsignificant for summer runoff.

309 **3.2. Estimation of groundwater storage by baseflow recession analysis**

310 Using the data selection procedure mentioned in the section 2.3.3, we adopted daily
311 streamflow and precipitation records in autumn and early winter (September to
312 December) in which the hydrograph with little precipitation usually declines



313 consecutively and smoothly. The fitted slope b is equal to 1.79 through the nonlinear
314 least square fit of equation (10) for all data points of $-dy/dt$ versus y in log-log space
315 during the period 1979-2013. Moreover, for each decade or year, the intercept a could
316 be fitted by the fixed slope $b=1.79$. Then, the values of K and m for each decade or
317 year can be determined. And the groundwater storage S for each year can be directly
318 estimated from the average rate of baseflow during a recession period through
319 equation (8).

320 Figure 8 shows the results of the nonlinear least square fit for each decade's
321 recession data from the 1980s, 1990s and 2000s, respectively. As shown in Figure 8,
322 the recession data points and fitted recession curves of each decade gradually move
323 downward as time goes on. This indicates that, with a fixed slope b , the intercept a
324 gradually decreases and recession coefficient K increases accordingly. The values of
325 recession coefficient K for each decade are $77 \text{ mm}^{0.79} \text{ d}^{0.21}$, $84 \text{ mm}^{0.79} \text{ d}^{0.21}$ and 103
326 $\text{mm}^{0.79} \text{ d}^{0.21}$. Furthermore, Figure 9a shows the inter-annual variation of recession
327 coefficient K during the period 1979-2013. In total, though there are some large
328 fluctuations or even a rather large decrease at the beginning of the 1990s, the overall
329 increasing trend of $7.70 (\text{mm}^{0.79} \text{ d}^{0.21})/10\text{a}$ at a significance level of 5% is similar to the
330 results obtained from decade analysis. This long-term variation of recession
331 coefficient K from September to December indicates that baseflow recession during
332 autumn and early winter gradually slows down in the catchment.

333 According to the results of decade data fit (see in Figure 8), the mean values of



334 groundwater storage S estimated for each decade are 130 mm, 148 mm and 188 mm
335 for the 1980s, 1990s and 2000s. The trend analysis suggests that the groundwater
336 storage S shows an increasing trend at the 5% significance level with a rate of about
337 19.32 mm/10a during the period 1979-2013 (Figure 9b). This indicates that
338 groundwater storage has been enlarged. The annual trend of groundwater storage S
339 from 1979 to 2013 is consistent with the values across decades. The inter-annual
340 variation of groundwater storage S is also similar with recession coefficient K (Figure
341 9a and 9b). The decreased trend of anomalies changes of groundwater storage (GWS)
342 estimated by the GRACE data is consistent with the annual trend of S during
343 2003~2015 (Figure 9b). And the reduced volume of groundwater between GWS and S
344 are also similar (~100-120 mm).

345 **4. Discussions**

346 The results have revealed that the increase of streamflow especially in dry season is
347 tightly related with climate warming. It is obviously that both glacier retreat and
348 frozen ground degradation in a warmer climate can significantly alter the mechanism
349 of streamflow. In the Yangbajain Catchment as well as the whole Lhasa River Basin,
350 it is experiencing a noticeable glacier retreat and frozen ground degradation during the
351 past decades (Table 3). For instance, according to the twice map of frozen ground
352 distribution on the TP (Li and Cheng, 1996; Zou et al., 2017), the areal extent of
353 permafrost in the Yangbajain catchment has decreased by 406 km² (15.3%) over the
354 past 22 years; the corresponding areal extent of seasonal frozen ground has increased



355 by 406 km² (15.3%) with the degradation of permafrost.

356 According to the new map of permafrost distribution on the Tibetan Plateau (Zou et
357 al., 2017), the coverages of permafrost and seasonally frozen ground in each
358 sub-catchment (especially the Lhasa sub-catchments) are comparable to that in the
359 Yangbajain Catchment; but the coverage of glaciers in the three catchments is far
360 lower than that in the Yangbajain Catchment according to the First Chinese Glacier
361 Inventory (Mi et al., 2002) (Table 3). The MK test showed that, in all the four
362 catchments, the annual mean air temperature had significant increases at the 1%
363 significance level (Figure 4) while the annual precipitation showed nonsignificant
364 trends (Table 4). The annual streamflow of the three Lhasa, Pangdo and Tangga
365 Catchments all had nonsignificant trends, while the annual streamflow of the
366 Yangbajain Catchment showed an increasing trend at the 5% significance level with a
367 mean rate of about 12.30 mm/10a during the period. Ye et al. (1999) stated that when
368 glacier coverage is greater than 5%, glacier contribution to streamflow starts to show
369 up. This indicates that, in the Yangbajain Catchment, the increased streamflow is
370 mainly fed by the accelerated glacier retreat rather than frozen ground degradation.
371 This conclusion is also consistent with previous results by Prasch et al. (2013), who
372 suggested that the contribution of accelerated glacial meltwater to streamflow would
373 bring a significant increase in streamflow in the Yangbajain Catchment. Thus it is
374 reasonable to attribute annual streamflow increases to the accelerated glacier retreat as
375 the consequence of increasing annual air temperature.



376 Although permafrost degradation is not the controlling factor for the increase of
377 streamflow, a rational hypothesis is that increased groundwater storage S in autumn
378 and early winter is associated with frozen ground degradation, which can enlarge
379 groundwater storage capacity (Niu et al., 2016). Figure 3 depicts the changes of
380 surface flow and groundwater flow paths in a glacier fed catchment, which is
381 underlain by frozen ground under past climate and warmer climate, respectively. As
382 frozen ground extent continues to decline and active layer thickness continues to
383 increase in the valley, the enlargement of groundwater storage capacity can provide
384 enough storage space to accommodate the increasing meltwater that may percolate
385 into deeper aquifers (Figure 3). Then, the increase of groundwater storage in autumn
386 and early winter allows more groundwater discharge into streams as baseflow, and
387 lengthens the recession time as indicated by recession coefficient K . This leads to the
388 increased baseflow and slow baseflow recession in autumn and early winter, as is
389 shown in Figure 6c, 6d and Figure 9a. In the late winter and spring, the increase of
390 baseflow (Figure 6d and 6a) can be explained by the delayed release of increased
391 groundwater storage.

392 Thus, as the results of climate warming, river regime in this catchment has been
393 altered significantly. On the one hand, permafrost degradation is changing the aquifer
394 structure that controls the storage-discharge mechanism, e.g., catchment groundwater
395 storage increases at about 19.32 mm/10a. On the other hand, huge amount of water
396 from glacier retreat is contributing to the increase of streamflow and groundwater



397 storage. For example, the annual streamflow of the Yangbajain Catchment increases
398 with a mean rate of about 12.30 mm/10a during the past 50 years. However, the total
399 glacial area and volume have decreased by 38.05 km² (12.0%) and 4.73×10⁹ m³
400 (26.2%) over the period 1960-2009 (Figure 10) according to the Chinese Glacier
401 Inventories. Hence, the reduction rate of glacial volume is 9.46×10⁷ m³/a (about 357.7
402 mm/10a) on average during the past 50 years. In the ablation on continental type
403 glaciers in China, evaporation (sublimation) always takes an important role, however,
404 annual amount of evaporation is usually less than 30% of the total ablation of glaciers
405 in the high mountains of China (Zhang et al., 1996). Given the 30% reduction in
406 glacial melt, there is still a large water imbalance between melt-derived runoff and the
407 actually increase of runoff and groundwater storage.

408 So the considerable water imbalance (estimated at least to be 5.79×10⁷ m³/a)
409 provides a perspective about the deep subsurface leakage through the fault zone in the
410 Yangbajain Catchment. Our results imply that more than 60% of glacial meltwater
411 would be lost by subsurface leakage. In fact, the north-south trending fault in the
412 Yangbajain Catchment plays a significant role on accessing groundwater flow through
413 deep pathway (Jiang et al., 2016).

414 **5. Conclusions**

415 In this study, the changes of hydro-meteorological variables were evaluated to
416 identify the main climatic factor for streamflow increases in the Yangbajain
417 Catchment, a sub-basin with the largest glacier coverage and a widespread frozen



418 ground in the Lhasa River Basin in the south-central TP. We analyzed the changes of
419 streamflow components through baseflow separation method. We quantified baseflow
420 recession and active groundwater storage in autumn and early winter by recession
421 flow analysis, and discussed the seasonal variations of baseflow in response to the
422 changes in active groundwater storage.

423 We find that the annual streamflow especially the annual baseflow increases
424 significantly, and the rising air temperature acts as a primary factor for the increased
425 runoff. The increased streamflow is mainly fed by the accelerated glacier retreat due
426 to climate warming. The decreased glacial volume has supplied large quantities of
427 glacial meltwater which recharge aquifers and reside in temporary storage during
428 summer, and then release as baseflow during the following seasons. Moreover, frozen
429 ground degradation would enlarge groundwater storage capacity, and then provide
430 more storage spaces for the meltwater. This can explain why baseflow volume
431 increases and baseflow recession slows down in autumn and early winter. At last we
432 find that there is a large water imbalance ($> 5.79 \times 10^7 \text{ m}^3/\text{a}$) between melt-derived
433 runoff and the actually increase of runoff and groundwater storage, which suggests
434 more than 60% of the reduction in glacial melt should be lost by subsurface leakage
435 through the fault zone in the Yangbajain catchment.

436 This study provides a fundamental understanding of the changes in streamflow and
437 groundwater storage under a warming climate. It is of great importance to predict the
438 effects of future climate changes on water resources and hydrological processes in



439 highly glacier-fed and large-scale frozen ground regions. More methods (e.g.,
440 hydrological isotopes) should be adopted to quantify the contribution of glaciers
441 meltwater and permafrost degradation to streamflow, and to explore the change of
442 groundwater storage capacity as frozen ground continues to degrade.

443 **Acknowledgements:**

444 This work was supported by the National Natural Science Foundation of China
445 (NSFC) (grants 91647108, 91747203), the Science and Technology Program of Tibet
446 Autonomous Region (2015XZ01432), and the Special Fund of the State Key
447 Laboratory of Hydrology-Water Resources and Hydraulic Engineering (no
448 20185044312).

449 **References**

- 450 Bayard, D., Stähli, M., Parriaux, A., and Flüher, H.: The influence of seasonally
451 frozen soil on the snowmelt runoff at two alpine sites in southern Switzerland,
452 *Journal of Hydrology*, 309(1), 66-84, doi:10.1016/j.jhydrol.2004.11.012, 2005.
- 453 Kooi, H., Ferguson, G., Bense, V. F.: Evolution of shallow groundwater flow systems
454 in areas of degrading permafrost, *Geophysical Research Letters*, 36(22):297-304,
455 2009.
- 456 Bense, V. F., Kooi, H., Ferguson, G., and Read, T.: Permafrost degradation as a
457 control on hydrogeological regime shifts in a warming climate, *Journal of*
458 *Geophysical Research Earth Surface*, 117, F03036, doi:10.1029/2011JF002143,
459 2012.
- 460 Bibi, S., Wang, L., Li, X. P., Zhou, J., Chen, D. L., and Yao, T. D.: Climatic and
461 associated cryospheric, biospheric, and hydrological changes on the Tibetan Plateau:
462 A review, *International Journal of Climatology*, 38, e1-e17, doi:10.1002/joc.5411,



- 463 2018.
- 464 Brutsaert, W., and Lopez, J. P.: Basin-scale geohydrologic drought flow features of
465 riparian aquifers in the southern Great Plains, *Water Resources Research*, 34(2),
466 233-240, 1998.
- 467 Brutsaert, W., and Nieber, J. L.: Regionalized drought flow hydrographs from a
468 mature glaciated plateau, *Water Resources Research*, 13(3), 637-643, 1977.
- 469 Brutsaert, W.: Long-term groundwater storage trends estimated from streamflow
470 records: Climatic perspective, *Water Resources Research*, 44(2), 114-125,
471 doi:10.1029/2007WR006518, 2008.
- 472 Buttle, J. M.: Mediating stream baseflow response to climate change: the role of basin
473 storage, *Hydrological Processes*, 32(1), doi:10.1002/hyp.11418, 2017.
- 474 Chapman, T.: A comparison of algorithms for stream flow recession and baseflow
475 separation, *Hydrological Processes*, 13, 701-714, 1999.
- 476 Cheng, G. D., and Wu, T. H.: Responses of permafrost to climate change and their
477 environmental significance, Qinghai-Tibet Plateau, *Journal of Geophysical*
478 *Research Earth Surface*, 112, F02S03, doi:10.1029/2006JF000631, 2007.
- 479 Cuo, L., Zhang, Y. X., Zhu, F. X., and Liang, L. Q.: Characteristics and changes of
480 streamflow on the Tibetan Plateau: A review, *Journal of Hydrology Regional*
481 *Studies*, 2, 49-68, doi:10.1016/j.ejrh.2014.08.004, 2014.
- 482 Duan, L., Man, X., Kurylyk, B.L., Cai, T.: Increasing winter baseflow in response to
483 permafrost thaw and precipitation regime shifts in northeastern China, *Water*, 9, 25,
484 doi:10.3390/w9010025, 2017.
- 485 Evans, S. G., and Ge, S.: Contrasting hydrogeologic responses to warming in
486 permafrost and seasonally frozen ground hillslopes, *Geophysical Research Letters*,
487 44, 1803-1813, doi:10.1002/2016GL072009, 2017.
- 488 Evans, S. G., Ge, S., and Liang, S.: Analysis of groundwater flow in mountainous,
489 headwater catchments with permafrost, *Water Resources Research*, 51, 9127-9140,



- 490 doi:10.1002/2014WR016259, 2015.
- 491 Evans, S. G., Ge, S., Voss, C. I., and Molotch, N. P.: The role of frozen soil in
492 groundwater discharge predictions for warming alpine watersheds, *Water*
493 *Resources Research*, 54, 1599-1615, 2018.
- 494 Gao, M., Chen, X., Liu, J., Zhang, Z., and Cheng, Q.: Using two parallel linear
495 reservoirs to express multiple relations of power-law recession curves, *Journal of*
496 *Hydrologic Engineering*, 04017013, doi:10.1061/(ASCE)HE.1943-5584.0001518,
497 2017.
- 498 Ge, S., J. McKenzie, C. Voss, and Wu, Q.: Exchange of groundwater and
499 surface-water mediated by permafrost response to seasonal and long term air
500 temperature variation, *Geophysical Research Letters*, 38, L14402,
501 doi:10.1029/2011GL047911, 2011.
- 502 Green, T. R., Taniguchi, M., Kooi, H., Gurdak, J. J., Allen, D. M., and Hiscock, K. M.,
503 et al.: Beneath the surface of global change: impacts of climate change on
504 groundwater, *Journal of Hydrology*, 405(3), 532-560,
505 doi:10.1016/j.jhydrol.2011.05.002, 2011.
- 506 Immerzeel, W. W., van Beek, L. P. H., and Bierkens, M. F. P.: Climate change will
507 affect the Asian water towers, *Science*, 328, 1382-1385, 2010.
- 508 Jiang, W., Han, Z., Zhang, J., and Jiao, Q.: Stream profile analysis, tectonic
509 geomorphology and neotectonic activity of the Damxung-Yangbajain Rift in the
510 south Tibetan Plateau, *Earth Surface Processes and Landforms*, 41(10), 1312-1326,
511 doi:10.1002/esp.3899, 2016.
- 512 Kang, S. C., Xu, Y. W., You, Q. L., Flügel, W. A., Pepin, N., and Yao, T. D.: Review of
513 climate and cryospheric change in the Tibetan Plateau, *Environmental Research*
514 *Letters*, 5(1), 015101, doi:10.1088/1748-9326/5/1/015101, 2010.
- 515 Käser, D., and D. Hunkeler.: Contribution of alluvial groundwater to the outflow of
516 mountainous catchments, *Water Resources Research*, 52, 680-697,



- 517 doi:10.1002/2014WR016730, 2016.
- 518 Kendall, M. G.: Rank Correlation Methods, 4th ed, Charles Griffin, London, pp. 196,
519 1975.
- 520 Kirchner, J.W.: Catchments as simple dynamical systems: catchment characterization,
521 rainfall-runoff modeling, and doing hydrology backward, *Water Resources*
522 *Research*, 45, W02429, doi:10.1029/2008WR006912, 2009.
- 523 Li, S., and Cheng, G.: Map of Frozen Ground on Qinghai-Xizang Plateau, Gansu
524 Culture Press, Lanzhou, 1996.
- 525 Lin, K. T., and Yeh, H. F.: Baseflow recession characterization and groundwater
526 storage trends in northern Taiwan, *Hydrology Research*, 48(6), 1745-1756, 2017.
- 527 Liu, J. S., Xie, J., Gong, T. L., Wang, D., and Xie, Y. H.: Impacts of winter warming
528 and permafrost degradation on water variability, upper Lhasa River, Tibet,
529 *Quaternary International*, 244(2), 178-184, doi:10.1016/j.quaint.2010.12.018, 2011.
- 530 Liu, J. T., Han, X. L., Chen, X., Lin, H., and Wang, A. H.: How well can the
531 subsurface storage-discharge relation be interpreted and predicted using the
532 geometric factors in headwater areas? *Hydrological Processes*, 30(25), 4826-4840,
533 doi:10.1002/hyp.10958, 2016.
- 534 Liu, Q. Q., Singh, V. P., and Xiang, H.: Plot erosion model using gray relational
535 analysis method, *Journal of Hydrologic Engineering*, 10, 288-294, 2005.
- 536 Liu, S. Y., Guo, W., and Xu, J., et al.: The Second Glacier Inventory Dataset of China
537 (Version 1.0), Cold and Arid Regions Science Data Center at Lanzhou, 2014,
538 doi:10.3972/glacier.001.2013.db.
- 539 Liu, X. D., and Chen, B. D.: Climatic warming in the Tibetan Plateau during recent
540 decades, *International Journal of Climatology*, 20(14), 1729-1742, 2000.
- 541 Lyne, V., and Hollick, M.: Stochastic time-variable rainfall-runoff modeling, Aust.
542 Natl. Conf. Publ. pp.89-93, 1979.
- 543 Lyon, S. W., and Destouni, G.: Changes in catchment-scale recession flow properties



- 544 in response to permafrost thawing in the Yukon River basin, *International Journal*
545 *of Climatology*, 30(14), 2138-2145, doi:10.1002/joc.1993, 2010.
- 546 Lyon, S. W., Destouni, G., Giesler, R., Humborg, C., Mörth, M., and Seibert, J., et al.:
547 Estimation of permafrost thawing rates in a sub-arctic catchment using recession
548 flow analysis, *Hydrology and Earth System Sciences Discussions*, 13(5), 595-604,
549 2009.
- 550 Mann, H.: Non-parametric test against trend, *Econometrica*, 13, 245-259, 1945.
- 551 Mi, D. S., Xie, Z. C., and Luo, X. R.: Glacier Inventory of China (volume XI: Ganga
552 River drainage basin and volume XII: Indus River drainage basin). Xi'an
553 Cartographic Publishing House, Xi'an, pp. 292-317, 2002 (In Chinese).
- 554 Niu, L., Ye, B. S., Li, J., and Sheng, Y.: Effect of permafrost degradation on
555 hydrological processes in typical basins with various permafrost coverage in
556 western China, *Science China Earth Sciences*, 54(4), 615-624,
557 doi:10.1007/s11430-010-4073-1, 2011.
- 558 Niu, L., Ye, B., Ding, Y., Li, J., Zhang, Y., Sheng, Y., and Yue, G.: Response of
559 hydrological processes to permafrost degradation from 1980 to 2009 in the upper
560 Yellow River basin, China, *Hydrology Research*, 47(5), 1014-1024,
561 doi:10.2166/nh.2016.096, 2016.
- 562 Prasher, M., Mauser, W., and Weber, M.: Quantifying present and future glacier
563 melt-water contribution to runoff in a central Himalayan river basin, *Cryosphere*,
564 7(3), 889-904, doi:10.5194/tc-7-889-2013, 2013.
- 565 Pritchard, H. D.: Asia's glaciers are a regionally important buffer against drought,
566 *Nature*, 545(7653), 169, doi:10.1038/nature22062, 2017.
- 567 Qin, Y., Lei, H., Yang, D., Gao, B., Wang, Y., Cong, Z., and Fan, W.: Long-term
568 change in the depth of seasonally frozen ground and its ecohydrological impacts in
569 the Qilian Mountains, northeastern Tibetan Plateau, *Journal of Hydrology*, 542,
570 204-221, 2016.



- 571 Richey, A. S., Thomas, B. F., Lo, M.-H., Reager, J. T., Famiglietti, J. S., Voss, K.,
572 Swenson, S., and Rodell, M.: Quantifying renewable groundwater stress with
573 GRACE, *Water Resources Research*, 51, 5217–5238, doi:10.1002/2015WR017349,
574 2015.
- 575 Rupp, D. E., and Selker, J. S.: Information, artifacts, and noise in $dQ/dt-Q$ recession
576 analysis, *Advances in Water Resources*, 29(2), 154-160, 2006.
- 577 Save, H., Bettadpur, S., and Tapley, B. D.: High - resolution CSR GRACE RL05
578 mascons, *Journal of Geophysical Research: Solid Earth*, 121, 7547–7569,
579 doi.org/10.1002/2016JB013007, 2016.
- 580 Singleton, M.J., and Moran, J.E.: Dissolved noble gas and isotopic tracers reveal
581 vulnerability of groundwater in a small, high elevation catchment to predicted
582 climate change, *Water Resources Research*, 46, W00F06,
583 doi:10.1029/2009WR008718, 2010.
- 584 Sjöberg, Y., Frampton, A., and Lyon, S. W.: Using streamflow characteristics to
585 explore permafrost thawing in northern Swedish catchments, *Hydrogeology Journal*,
586 21, 121-131, 2013.
- 587 Smith, L. C., Pavelsky, T. M., Macdonald, G. M., Shiklomanov, A. I., Lammers, R. B.:
588 Rising minimum daily flows in northern Eurasian rivers: A growing influence of
589 groundwater in the high-latitude hydrologic cycle, *Journal of Geophysical Research*
590 *Biogeosciences*, 112, G04S47, doi:10.1029/2006JG000327, 2007.
- 591 St. Jacques, J. M. S., and Sauchyn, D. J.: Increasing winter base flow and mean
592 annual streamflow from possible permafrost thawing in the northwest Territories,
593 Canada, *Geophysical Research Letters*, 36(1), 329-342,
594 doi:10.1029/2008GL035822, 2009.
- 595 Staudinger, M., Stoelzle, M., Seeger, S., Seibert, J., Weiler, M., and Stahl, K.:
596 Catchment water storage variation with elevation, *Hydrological Processes*, 31(11),
597 doi:10.1002/hyp.11158, 2017.



- 598 Viviroli, D., Du ir, H. H., Messerli, B., Meybeck, M., and Weingartner, R.: Mountains
599 of the world, water towers for humanity: Typology, mapping, and global
600 significance, *Water Resources Research*, 43, W07447, doi:10.1029/2006WR005653,
601 2007.
- 602 Walvoord, M. A., and Kurylyk, B. L.: Hydrologic impacts of thawing permafrost-A
603 review, *Vadose Zone Journal*, 15(6), doi:10.2136/vzj2016.01.0010, 2016.
- 604 Walvoord, M. A., and Striegl, R. G.: Increased groundwater to stream discharge from
605 permafrost thawing in the Yukon River basin: Potential impacts on lateral export of
606 carbon and nitrogen, *Geophysical Research Letters*, 34(12), 123-134,
607 doi:10.1029/2007GL030216, 2007.
- 608 Wang, G., Mao, T., Chang, J., Song, C., and Huang, K.: Processes of runoff
609 generation operating during the spring and autumn seasons in a permafrost
610 catchment on semi-arid plateaus, *Journal of Hydrology*, 550, 307-317, 2017.
- 611 Wang, S., Liu, S. X., Mo, X. G., Peng, B., Qiu, J. X., Li, M. X., Liu, C. M., Wang, Z.
612 G., and Bauer-Gottwein, P.: Evaluation of remotely sensed precipitation and its
613 performance for streamflow simulations in basins of the southeast Tibetan Plateau,
614 *Journal of Hydrometeorology*, 16(6), 342-354, doi:10.1175/JHM-D-14-0166.1,
615 2015.
- 616 Wang, Y. F., Shen, Y. J., Chen, Y. N., and Guo, Y.: Vegetation dynamics and their
617 response to hydroclimatic factors in the Tarim River Basin, China, *Ecohydrology*,
618 6(6), 927-936, 2013.
- 619 Wittenberg, H.: Baseflow recession and recharge as nonlinear storage processes,
620 *Hydrological Processes*, 13, 715-726, 1999.
- 621 Woo, M. K., Kane, D. L., Carey, S. K., and Yang, D.: Progress in permafrost
622 hydrology in the new millennium, *Permafrost & Periglacial Processes*, 19(2),
623 237-254, doi:10.1002/ppp.613, 2008.
- 624 Wu, Q. B., and Zhang, T. J.: Recent permafrost warming on the Qinghai-Tibetan



- 625 Plateau, *Journal of Geophysical Research Atmospheres*, 113, D13108,
626 doi:10.1029/2007JD009539, 2008.
- 627 Wu, Z. H., and Zhao, X. T.: Quaternary geology and faulting in the
628 Damxung-Yangbajain Basin, southern Tibet, *Journal of Geomechanics*, 12(3),
629 305-316, 2006 (in Chinese).
- 630 Yang, G., Lei, D., Hu, Q., Cai, Y., and Wu, J.: Cumulative coulomb stress changes in
631 the basin-range region of Gulu-Damxung-Yangbajain and their effects on strong
632 earthquakes, *Electronic Journal of Geotechnical Engineering*, 22(5), 1523-1530,
633 2017.
- 634 Yao, T. D., Pu, J. C., Lu, A. X., Wang, Y. Q., and Yu, W. S.: Recent glacial retreat and
635 its impact on hydrological processes on the Tibetan Plateau, China, and
636 surrounding regions, *Arctic, Antarctic, and Alpine Research*, 39(4), 642-650, 2007.
- 637 Yao, T. D., Wang, Y. Q., Liu, S. Y., Pu, J. C., Shen, Y. P., and Lu, A. X.: Recent glacial
638 retreat in high Asia in China and its impact on water resource in northwest China,
639 *Science in China*, 47(12), 1065-1075, doi:10.1360/03yd0256, 2004.
- 640 Ye, B. S., Han, T. D., Ding, Y. J.: Some Changing Characteristics of Glacier
641 Streamflow in Northwest China, *Journal of Glaciology and Geocryology*,
642 21(1):54-58, 1999 (in Chinese).
- 643 Yue, S., Pilon, P., Phinney, B., and Cavadias, G.: The influence of autocorrelation on
644 the ability to detect trend in hydrological series, *Hydrological Processes*, 16(9),
645 1807-1829, doi:10.1002/hyp.1095, 2002.
- 646 Zhang, Y., Yao, T. D., and Pu, J. C.: The characteristics of ablation on continental-type
647 glaciers in China, *Journal of Glaciology and Geocryology*, 18(2), 147-154, 1996 (in
648 Chinese).
- 649 Zhang, Y., Wang, C., and Bai, W., et al.: Alpine wetland in the Lhasa River Basin,
650 China, *Journal of Geographical Sciences*, 20(3): 375-388, 2010 (in Chinese).
- 651 Zhou, Y. W., Guo, D. X., Qiu, G. Q., Cheng, G. D., and Li, S. D.: Permafrost in China,



652 Science Press, Beijing, pp. 63-70, 2000 (In Chinese).
653 Zou, D., Zhao, L., Sheng, Y., and Chen, J., et al.: A new map of permafrost
654 distribution on the Tibetan Plateau, *The Cryosphere*, 11, 2527-2542,
655 doi:10.5194/tc-11-2527-2017, 2017.
656



657

Table 1. Mann-Kendall trend test with trend-free pre-whitening of seasonal and annual mean air temperature ($^{\circ}\text{C}$), precipitation (mm), streamflow (mm), baseflow (mm) and quick flow (mm) from 1979 to 2013.

	Air temperature		Precipitation		Streamflow		Baseflow		Quick flow	
	Z_c	β ($^{\circ}\text{C}/\text{a}$)	Z_c	β (mm/a)	Z_c	β (mm/a)	Z_c	β (mm/a)	Z_c	β (mm/a)
Spring	2.73**	0.026	0.90	0.290	3.05**	0.206	2.99**	0.147	0.98	0.042
Summer	2.63**	0.013	1.30	2.139	0.92	0.549	1.27	0.429	0.50	0.128
Autumn	2.65**	0.024	-0.68	-0.395	2.46*	0.546	2.96**	0.476	0.80	0.074
Winter	3.49**	0.051	-0.46	-0.014	3.08**	0.204	2.13*	0.145	1.39	0.016
Annual	4.48**	0.028	1.28	2.541	2.07*	1.230	2.70**	1.095	0.77	0.327

Comment: the symbols of Z_c and β mean the standardized test statistic and the trend magnitude, respectively; positive values of Z_c and β indicate the upward trend, whereas negative values indicate the downward trend in the tested time series; the symbols of asterisks *and ** mean statistically significant at the levels of 5% and 1%, respectively.

Table 2. Gray relational grades between the streamflow/baseflow and climate factors (precipitation and air temperature) in the Yangbajain Catchment at both annual and seasonal scales. Bold text shows the higher gray relational grade in each season.

	G_{oi} with the streamflow		G_{oi} with the baseflow	
	Precipitation	Air temperature	Precipitation	Air temperature
Spring	0.690	0.778	0.713	0.789
Summer	0.689	0.784	0.680	0.776
Autumn	0.653	0.667	0.648	0.680
Winter	0.742	0.886	0.748	0.895
Annual	0.675	0.727	0.665	0.729

Comment: G_{oi} is the gray relational grade between the streamflow/baseflow and climate factors. The importance of each influence factor can be determined by the order of the gray relational grade values. The influence factor with the largest G_{oi} is regarded as the main stress factor for the objective variable.

658
659



660 Table 3. The coverage of glaciers and frozen ground in four catchments of the Lhasa River Basin

Stations	Glaciers(1960)		Glaciers(2009)		Permafrost (1996)		Permafrost (2017)		Seasonally frozen ground (1996)		Seasonally frozen ground (2017)	
	Area (km ²)	Coverage (%)	Area (km ²)	Coverage (%)	Area (km ²)	Coverage (%)						
Lhasa	26233	1.3	347.14	1.3	10535	40.2	9783	37.3	15698	59.8	16450	62.7
Pangdo	16425	2.1	339.90	2.1	8666	52.7	8242	50.2	7762	47.3	8184	49.8
Tangga	20152	1.7	342.27	1.7	10081	50.0	9432	46.8	10071	50.0	10720	53.2
Yangbajain	2645	12.0	278.26	10.5	1352	51.1	946	35.8	1293	48.9	1699	64.2

661

662 Table 4. Mann-Kendall trend test with trend-free pre-whitening of annual mean air temperature (°C), precipitation (mm) and streamflow (mm) in
 663 four catchments of the Lhasa River Basin

	Air temperature		Precipitation		Streamflow	
	Z _C	β (°C/a)	Z _C	β (mm/a)	Z _C	β (mm/a)
Lhasa	6.07**	0.028	1.16	1.581	1.09	1.420
Pangdo	6.19**	0.026	0.89	1.435	0.30	0.223
Tangga	7.35**	0.021	1.48	2.005	-0.62	-0.531
Yangbajain	4.48**	0.028	1.28	2.541	2.07*	1.230

664



665 **Figure captions**

666 **Figure 1.** (a) The location, (b) elevation distribution, and (c) glacier and frozen
667 ground distribution (Zou et al., 2017) in the Yangbajain Catchment of the Lhasa River
668 Basin in the TP.

669 **Figure 2.** Seasonal variation of streamflow (R), mean air temperature (T), and
670 precipitation (P) in the Yangbajain Catchment.

671 **Figure 3.** Diagram depicting surface flow and groundwater flow due to glacier melt
672 and frozen ground thaw under (a) past climate and (b) warmer climate. Blue lines
673 with arrows are conceptual surface flow paths. Red lines with arrows are conceptual
674 groundwater flow paths (after Evans and Ge. (2017)).

675 **Figure 4.** Variations of annual (a) streamflow and (b) baseflow from 1979 to 2013.

676 **Figure 5.** Variations of annual (a) mean air temperature and (b) precipitation from
677 1979 to 2013.

678 **Figure 6.** Variations of seasonal streamflow and baseflow in (a) spring, (b) summer,
679 (c) autumn, and (d) winter from 1979 to 2013.

680 **Figure 7.** Variations of seasonal mean air temperature in (a) spring, (b) summer, (c)
681 autumn, and (d) winter from 1979 to 2013.

682 **Figure 8.** Recession data points of $-dy/dt$ versus y and fitted recession curves by
683 decades in log-log space. The black point line, dotted line, and solid line represent
684 recession curves in the 1980s, 1990s, and 2000s, respectively.

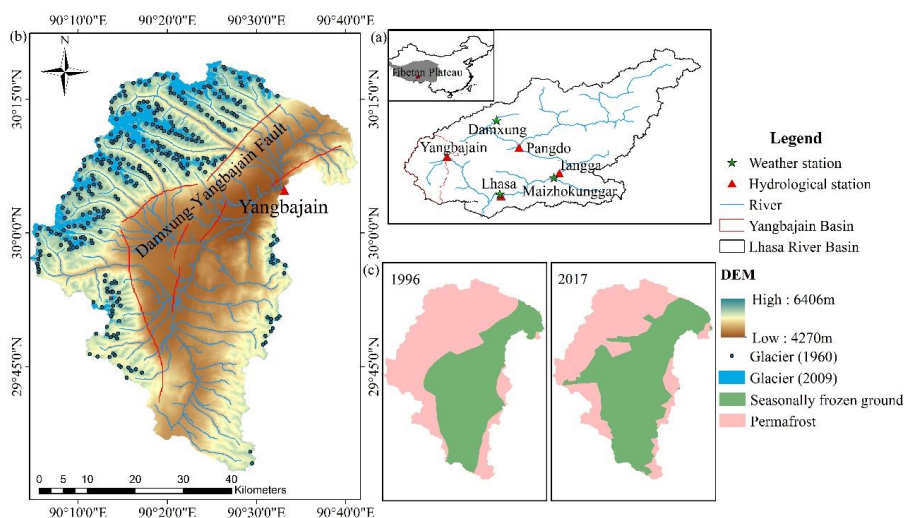
685 **Figure 9.** Variations of (a) the recession coefficient K and (b) groundwater storage S



686 from 1979 to 2013.

687 **Figure 10.** The total area and volume of glaciers in the Yangbajain Catchment in 1960

688 and 2009.



689

690 **Figure 1.** (a) The location, (b) elevation and glacier distribution for the twice Chinese

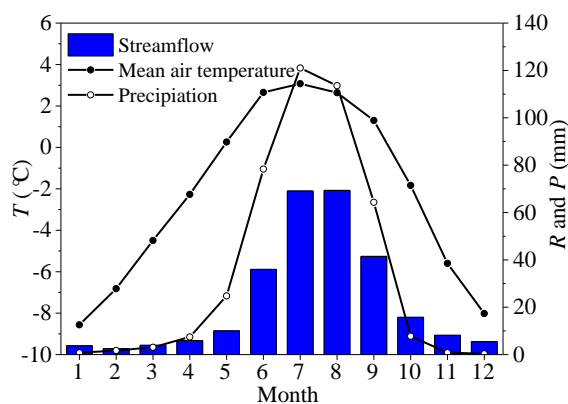
691 Glacier Inventory, only the location of glacier snouts in 1960 were provided in the

692 first Chinese Glacier Inventory, and the boundaries of glaciers were shown in the

693 second Chinese Glacier Inventory, and (c) twice maps of frozen ground distribution

694 (Li and Cheng, 1996; Zou et al., 2017) in the Yangbajain Catchment.

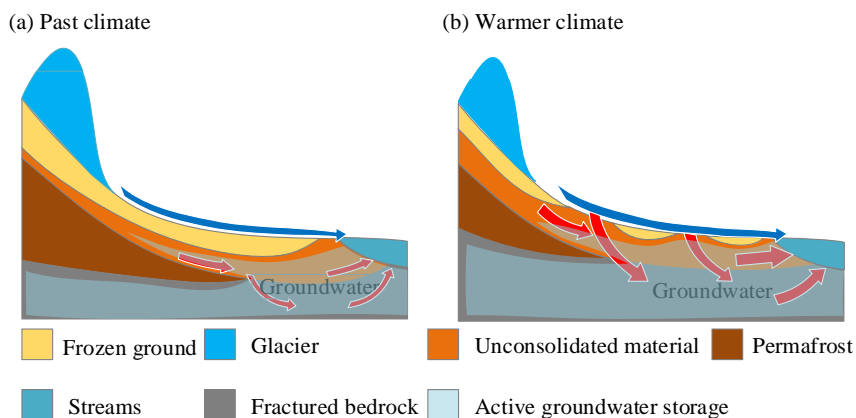
695



696

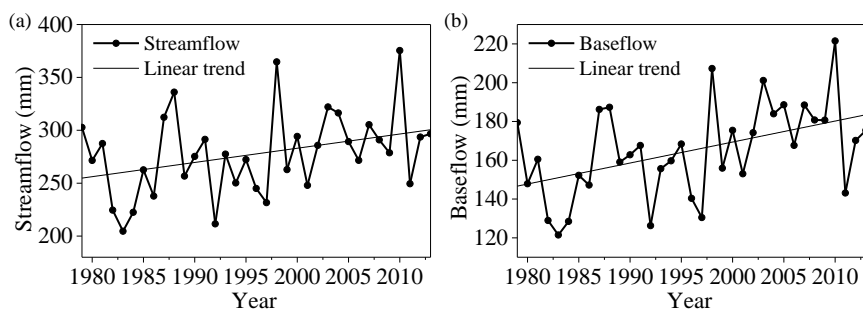
697 **Figure 2.** Seasonal variation of streamflow (R), mean air temperature (T), and
 698 precipitation (P) in the Yangbajain Catchment.

699



700

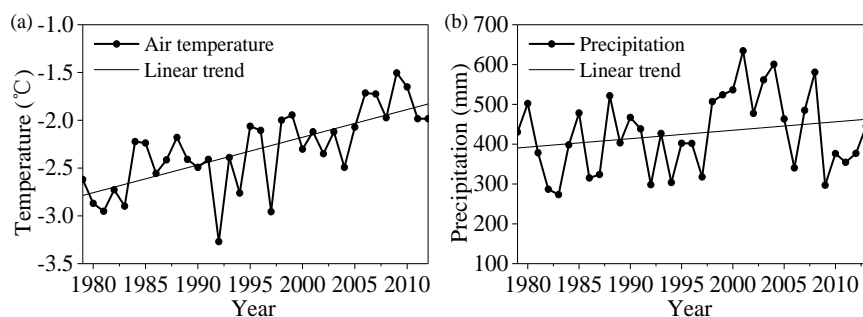
701 **Figure 3.** Diagram depicting surface flow and groundwater flow due to glacier melt
 702 and frozen ground thaw under (a) past climate and (b) warmer climate. Blue lines
 703 with arrows are conceptual surface flow paths. Red lines with arrows are conceptual
 704 groundwater flow paths (after Evans and Ge. (2017)).



705

706 **Figure 4.** Variations of annual (a) streamflow and (b) baseflow from 1979 to 2013.

707



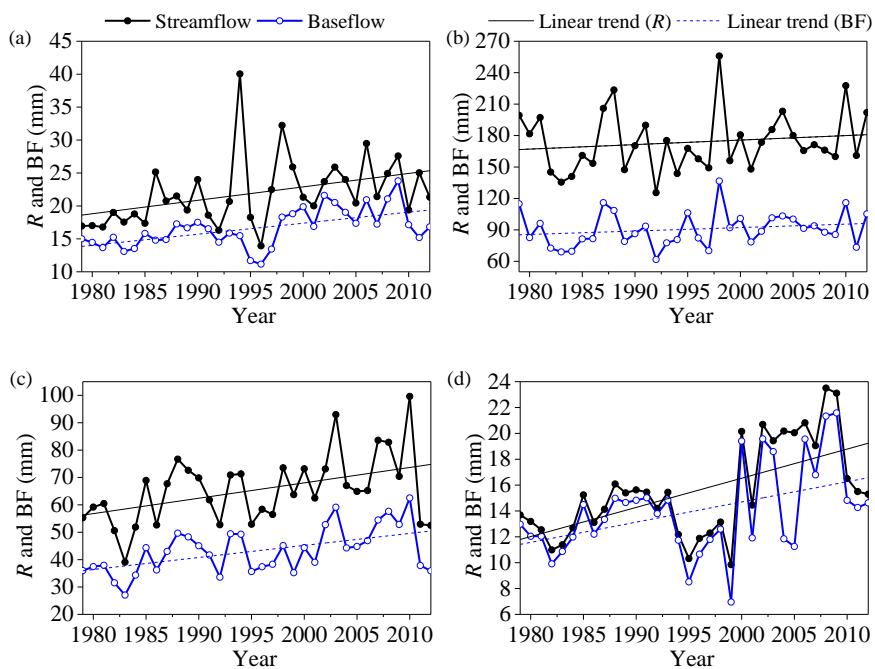
708

709 **Figure 5.** Variations of annual (a) mean air temperature and (b) precipitation from

710

1979 to 2013.

711



712

713

714

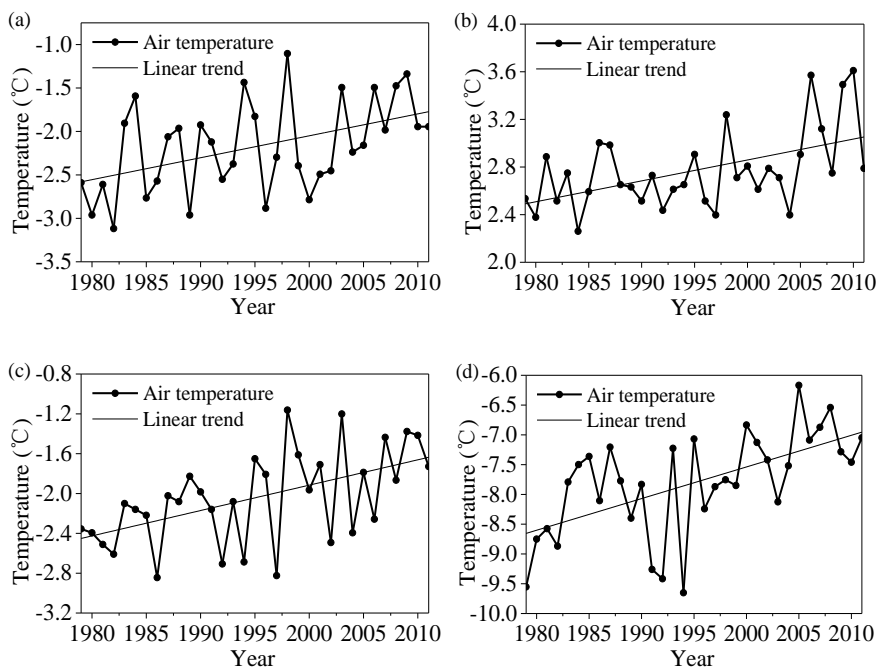
Figure 6. Variations of seasonal streamflow and baseflow in (a) spring, (b) summer,

715

(c) autumn, and (d) winter from 1979 to 2013.

716

717



718

719

720

Figure 7. Variations of seasonal mean air temperature in (a) spring, (b) summer, (c)

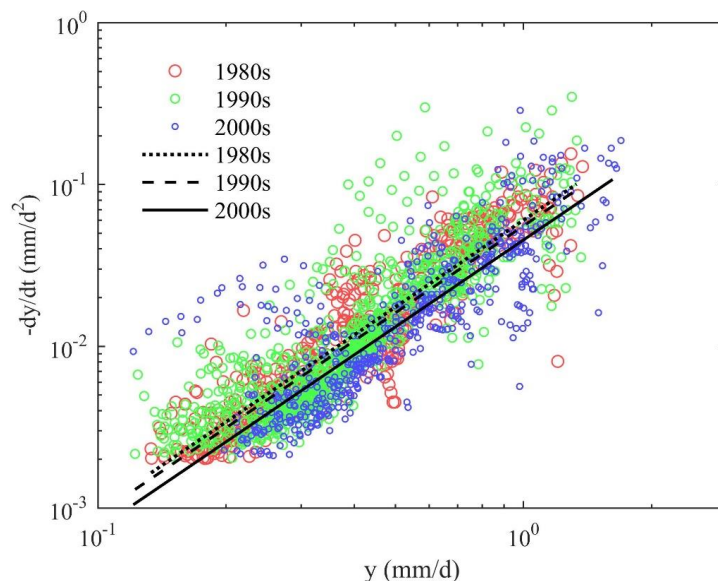
721

autumn, and (d) winter from 1979 to 2013.

722



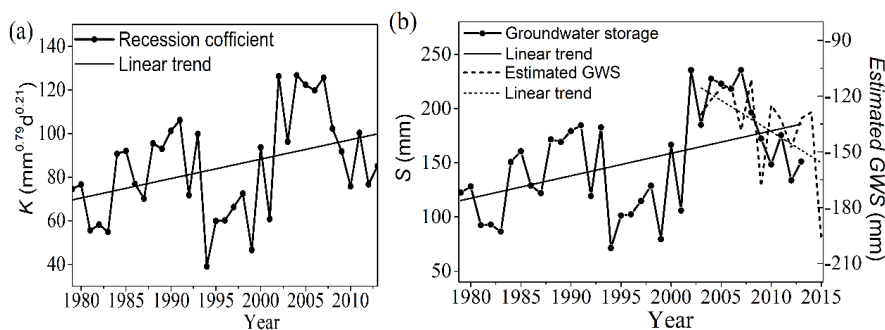
723



724

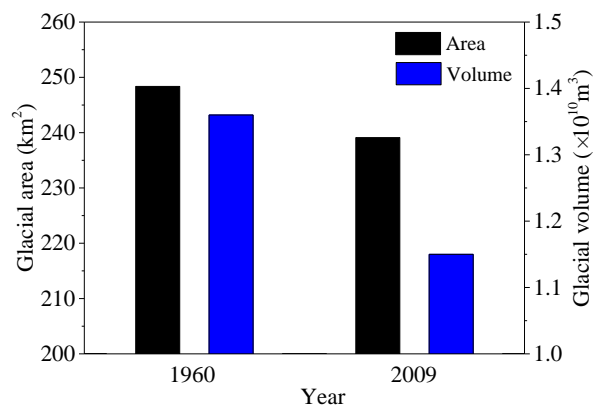
725 **Figure 8.** Recession data points of $-dy/dt$ versus y and fitted recession curves by
 726 decades in log-log space. The black point line, dotted line, and solid line represent
 727 recession curves in the 1980s, 1990s, and 2000s, respectively.

728



729

730 **Figure 9.** Variations of (a) the recession coefficient K and (b) the estimated
 731 groundwater storage S from 1979 to 2013 and the estimated groundwater storage
 732 change from 2003 to 2015 by GRACE data.



733

734

Figure 10. The total area and volume of glaciers in the Yangbajain Catchment in

735

1960 and 2009.

736